This is the peer-reviewed version of the chapter:

Radonjić, A., Sovilj, P., Đorđević Kozarov, J., Vujičić, V., 2019. Stochastic Digital Measurement Method and Its Application in Signal Processing, in: Advances in Engineering Research. Volume 27. Nova Science Publishers, Hauppauge, pp. 169–190. ISBN 978-1-5361-4803-9

Chapter

Stochastic Digital Measurement Method and Its Application in Signal Processing

Aleksandar Radonjic*

Institute of Technical Sciences of the Serbian Academy of Sciences and Arts, Belgrade, Serbia

Platon Sovilj

Faculty of Technical Sciences, University of Novi Sad, Novi Sad, Serbia

Jelena Djordjevic-Kozarov

Faculty of Electronic Engineering, University of Nis, Nis, Serbia

Vladimir Vujicic

Institute of Technical Sciences of the Serbian Academy of Sciences and Arts, Belgrade, Serbia

ABSTRACT

Classical measurement approach is often described as a process of discretizing an analogue signal in order to easily process it in some type of digital signal processor. Although this approach has been considered to be universally applicable, practical experience has shown that some signals (e.g. fast and/or noisy signals) cannot be always precisely measured. To overcome this problem, in the late 1990s, a new measurement approach called stochastic digital measurement method (SDMM) was presented. At the beginning, this method was intended for high-precision measurements of the integral (the mean value) of a product of two signals. However, in the late 2000s, it was shown that SDMM can be used to compute the Discrete Fourier Transform (DFT). Compared to the classical DFT/FFT processors, SDMM-based ones have two important advantages: first, they are much simpler and cheaper to implement, and second, they allow us to compute individual DFT components either in isolation or in parallel. This chapter is a review of the evolution of SDMM with a special emphasis on a two-bit SDMM. Topics covered include: theoretical foundations of SDMM, the architecture of SDMM-DFT processor and an example of prototype instrument used in power grid networks.

Keywords: Stochastic measurements, Fourier coefficients, DFT processor, signal processing.

* Corresponding Author address
Email: sasa_radonjic@yahoo.com

1. INTRODUCTION

The term “measurement”, is almost always considered to be a discrete digital measurement, i.e. the measurement in a point. In the metrology jargon this is called the sampling measurement method (SMM). Although very popular, the SMM has two inherent sources of systematic measurement error: the discretization in time and the discretization in value. If the sampling theorem conditions are satisfied, the discretization in time is eliminated as a source of measurement error. However, the discretization in value always causes a systematic measurement error. In other words, it cannot be eliminated, but only reduced to an acceptable value.

The essence of the sampling method is as follows: in a theoretically infinitely short time interval, a sample of an analogue measured variable is taken and in the time interval Δt, this sample is converted into a number, in a device called analog-to-digital converter (ADC). The time interval Δt is related to a sampling frequency f_s, and must satisfy the equality

$$\frac{1}{\Delta t} = f_s = 2 \cdot f_g \tag{1}$$

where f_g is the highest frequency which appears in the measured signal, i.e. the upper limit of the frequency band of the measured signal.

In practice, it is often needed to capture fast-changing signals, i.e. signals where $\Delta t < 1$ *ns*. For that purpose one uses flash ADCs, which perform the conversion within a single clock cycle and hence achieve $\Delta t < 1$ *ns*. However, the drawback of flash ADCs is that they represent compromise between the resolution (the number of bits) and hardware complexity. The resolution of modern flash ADCs is up to 10 bits. On the other hand, it is known that every additional bit of resolution doubles the hardware complexity. From that point of view, it is desirable to have a lower resolution. However, if the resolution is below 7 bits, the Bennett model of quantization error does not apply any more [2]. In such a case the quantization error cannot be treated as a white noise, which becomes a serious theoretical and practical problem.

In view of the above, it is natural to ask whether is it possible to measure fast and/or noisy signals accurately? Fortunately, the answer is positive if one uses stochastic digital measurement method (SDMM).

2. STOCHASTIC DIGITAL MEASUREMENT METHOD (SDMM)

The measurement on a finite time interval or SDMM is developed to overcome the limitations of SMM [3]. At the same time, it preserves almost all the advantages of SMM, especially the huge amount of software developed over the years in all branches of science and technology.

The advantages of SDMM are:

- measurement at high frequencies,
- measurement of noisy signals,
- high linearity and low uncertainty of measurement.

These features often appear simultaneously and can provide high-accuracy results in areas where it was not possible before [4-16].

2.1. One-channel SDMM

The main idea of SDMM consists in adding a random uniform dither $h(t)$ to the input signal $f(t)$ before its digitalization [3]. The dither signal is in the range of one quantum of the flash ADC and its average value is zero. In other words, the following conditions must be met:

a) $|f(t)+h(t)| \le R+\Delta/2,$ (2)

b) $|f(t)| \le R,$ (3)

c) $|h(t)| \le \Delta/2,$ (4)

d) $p(h)=1/\Delta,$ (5)

where $R = \Delta\cdot(2^m - 1)$ is the range of the flash ADC, m is a number of quantum levels, Δ is a quantum of the flash ADC and $p(h)$ is the probability density function of the signal $h(t)$. If, during the measurement interval $T = t_1 - t_2$, N conversions are performed, the accumulator from Fig. 1 will accumulate a series of samples $\Psi(i)$, where $1 \le i \le N$. The average value of these samples will be equal to [3]

$$\bar{\Psi} = \frac{1}{N}\cdot\sum_{i=1}^{N}\Psi(i) \approx \frac{1}{t_2-t_1}\int_{t_1}^{t_2} f(t)\,dt \tag{6}$$

whereas the variance of the average error e will not be greater than

$$\sigma_{\bar{e}}^2 \le \frac{1}{N}\cdot\left[\frac{\Delta}{t_2-t_1}\int_{t_1}^{t_2}|f(t)|dt - \frac{1}{t_2-t_1}\int_{t_1}^{t_2} f^2(t)\,dt\right] \tag{7}$$

i.e. it will be not greater than

$$\sigma_{\bar{e}}^2 \le \frac{1}{N}\cdot\left[\frac{R}{t_2-t_1}\int_{t_1}^{t_2}|f(t)|dt - \frac{1}{t_2-t_1}\int_{t_1}^{t_2} f^2(t)\,dt\right] \tag{8}$$

if a two-bit flash ADC is used. From (6) we conclude that one-channel SDMM instrument (Fig. 1) measures the average value of the signal $f(t)$. A modified version of this instrument (Fig. 2) can measure the absolute mean value of the signal $f(t)$

$$\bar{\Psi} = \frac{1}{N}\cdot\sum_{i=1}^{N}\Psi(i) \approx \frac{1}{t_2-t_1}\int_{t_1}^{t_2}|f(t)|dt \tag{9}$$

with the same upper bound for $\sigma_{\bar{e}}^2$ as in (8).

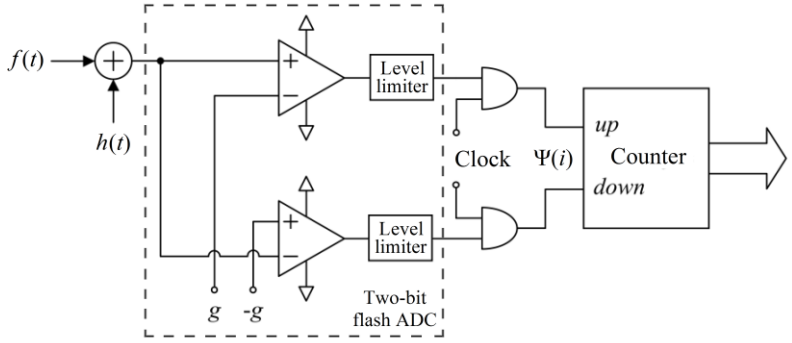

Fig. 1. A two-bit scheme for measuring the average value of the signal $f(t)$.

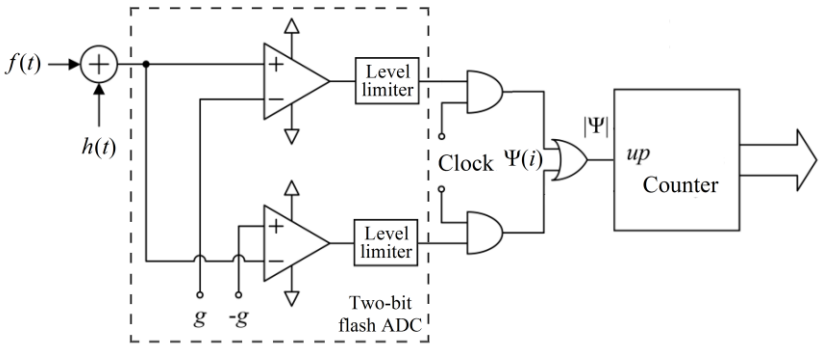

Fig. 2. A two-bit scheme for measuring the absolute mean value of the signal $f(t)$.

From the above, it can be concluded that the measurement accuracy can be improved by increasing the measurement time interval and/or sampling frequency. In other words, to achieve excellent measurement accuracy, it is sufficient to use fast two-bit flash ADCs!

2.2. Two-channel SDMM

There are applications in which it is necessary to calculate the mean value of a product of two physical quantities (e.g. voltage and current, flow and temperature, force and velocity, etc.). This problem can be solved by applying a two-channel SDMM. Unlike one-channel scheme, this one implies the use of four signals satisfying the conditions:

e) $|f_i(t)+h_i(t)| \le R_i + \Delta_i/2,$ (10)

f) $|f_i(t)| \le R_i,$ (11)

g) $|h_i(t)| \le \Delta_i/2,$ (12)

h) $p(h_i) = 1/\Delta_i,$ (13)

where i = 1, 2, $R_i = \Delta_i \cdot (2^m - 1)$ is the range of the flash ADC$_i$, Δ_i is a quantum of the flash ADC$_i$ and $p(h_i)$ is the probability density function of the signal $h_i(t)$. If the signals $h_1(t)$ and $h_2(t)$ are mutually uncorrelated, the instrument's output value (Fig. 3) will be equal to [5]

$$\bar{\Psi} = \frac{1}{N} \cdot \sum_{i=1}^{N} \Psi_1(i) \cdot \Psi_2(i) \approx \frac{1}{t_2 - t_1} \int_{t_1}^{t_2} f_1(t) \cdot f_2(t)\, dt \tag{14}$$

whereas the variance of the average error e will not be greater than

$$\sigma_{\bar{e}}^2 \le \frac{1}{N} \cdot \left[\frac{{\Delta_1}^2}{4 \cdot (t_2 - t_1)} \cdot \int_{t_1}^{t_2} f_2^2(t)\, dt + \frac{{\Delta_2}^2}{4 \cdot (t_2 - t_1)} \cdot \int_{t_1}^{t_2} f_1^2(t)\, dt + \frac{{\Delta_1}^2 \cdot {\Delta_2}^2}{16} \right] \tag{15}$$

If both flash ADCs have two-bit resolution ($\Delta_1 = \Delta_2 = R$), the above inequality reduces to

$$\sigma_{\bar{e}}^2 \le \frac{1}{N} \cdot \left[\frac{R^2}{4 \cdot (t_2 - t_1)} \cdot \int_{t_1}^{t_2} f_2^2(t)\, dt + \frac{R^2}{4 \cdot (t_2 - t_1)} \cdot \int_{t_1}^{t_2} f_1^2(t)\, dt + \frac{R^4}{16} \right] \tag{16}$$

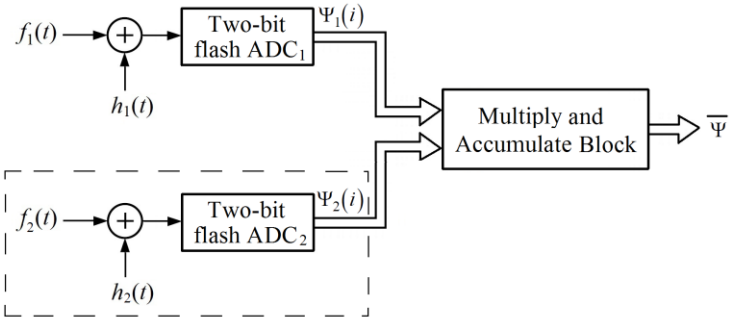

Fig. 3. A two-bit scheme for measuring the mean value of a product of the signals $f_1(t)$ and $f_2(t)$.

Another interesting application of two-channel SDMM is the measurement of the signal frequency. This can be done by combining SDMM with finite impulse response (FIR) filtering and digital zero crossing detection (DZCD) (Fig. 4). As described in [11], after digitalization, the output samples $f(n)$ are sent to the M-th order FIR filter, which performs a discrete convolution of the $f_1(n)$ with a set of coefficients $c(m)$

$$\hat{f}_1(n) = \sum_{m=0}^{M} c(m) \cdot f_1(n-m). \tag{17}$$

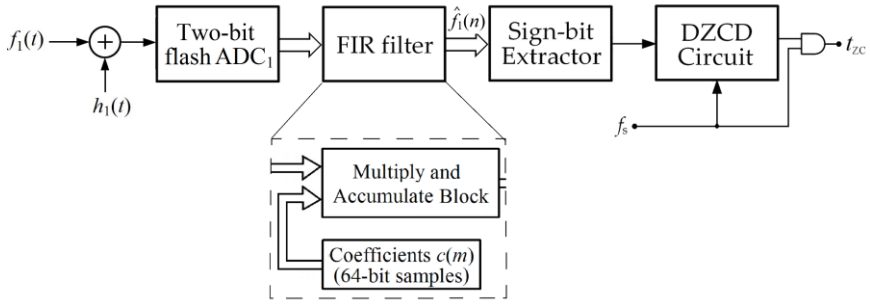

Fig. 4. The measurement of power grid frequency from the perspective of two-channel SDMM.

If the process of generating the signal $\hat{f}_1(n)$ is observed from the perspective of individual sample $\hat{f}_1$, it is clear that for sufficiently large M it holds that

$$\hat{f}_1 \approx \int_0^M c(m)\cdot f_1(const.-m)\,dm = \int_0^M c(m)\cdot v(m)\,dm. \tag{18}$$

The above approximation allows us to apply the theory behind two-channel SDMM. In other words, if $c(m)$ and $v(m)$ are two integrable functions over the interval [0, M], the variance of the average error e must satisfy the inequality

$$\sigma_{\bar{e}}^2 \le \frac{1}{M+1}\cdot\left[\frac{\Delta_{\mathrm{FIR}}^2}{4}\cdot\sum_{m=0}^{M} v^2(m) + \frac{R^2}{4}\cdot\sum_{m=0}^{M} c^2(m) + \frac{\Delta_{\mathrm{FIR}}^2\cdot R^2}{16}\cdot M\right] \tag{19}$$

Although the expression (19) might seem complicated, it can be significantly reduced if the coefficients $c(m)$ are memorized in a high-bit resolution. For instance, if the coefficients $c(m)$ are stored as 64-bit numbers, the value of the parameter Δ_{FIR} will be extremely small ($\Delta^2_{\mathrm{FIR}} \approx 10^{-38}$), and consequently, (19) becomes

$$\sigma_{\bar{e}}^2 \le \frac{1}{M+1}\cdot\left[\frac{R^2}{4}\cdot\sum_{m=0}^{M} c^2(m)\right] \tag{20}$$

If the FIR filter is well designed, the filtered signal will closely approximate a discrete sinusoidal function $s(n) = U_1\cdot sin(\omega n)$. In that case, if a coverage factor of $k = 2$ is used, the difference $d(n)$ between the $\hat{f}_1(n)$ and $s(n)$ will satisfy the inequality

$$\left|d(n)\right| = \left|U_1\cdot sin\left(\omega\cdot(n\pm\delta n)\right) - U_1\cdot sin(\omega n)\right| \approx U_1\cdot\omega\cdot|\delta n| \le 2\sigma_{\bar{e}} = R\cdot\left\lceil\sqrt{\frac{\sum_{m=0}^{M} c^2(m)}{M+1}}\right\rceil \tag{21}$$

where $\delta n \approx 0$ denotes a fixed time interval in which the filter signal $\hat{u}(n)$ may oscillate around zero. As the total number of oscillations N_s depends only on the sampling frequency f_s, it follows that

$$N_s \le \left\lceil\frac{R\cdot f_s}{U_1\cdot\omega}\cdot\sqrt{\frac{\sum_{m=0}^{M} c^2(m)}{M+1}}\right\rceil. \tag{22}$$

From this it is easy to conclude that the process of determination of the zero crossing instants is reduced to the detection of two binary sequences: 00…01 and 11…10. The circuit that performs

this function (DZCD circuit) is extremely simple: it consists of one (N_s+1)-bit shift register, two (N_s+1)-bit AND gates and one two-bit OR gate (Fig. 5).

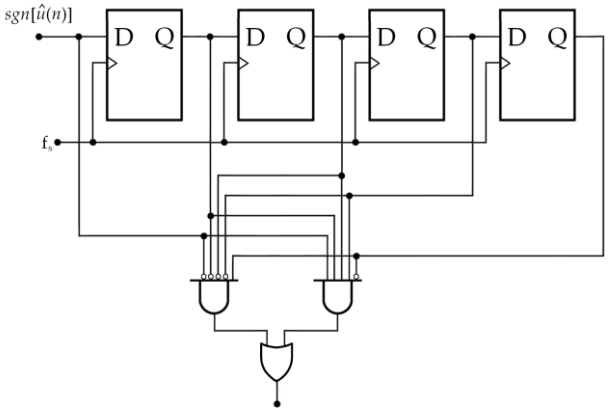

Fig. 5. Hardware implementation of DZCD circuit for $N_s = 4$.

3. STOCHASTIC DFT PROCESSOR

3.1. Circuit Architecture and Theory of Operation

From [1] it is well known that any periodic and continuous signal (with period T) can be approximated by the trigonometric polynomial of order *M*

$$f_1(t) \approx \frac{a_0}{2} + \sum_{i=1}^{M} [a_i \cdot \cos(i\omega t) + b_i \cdot \sin(i\omega t)] \tag{23}$$

where the Fourier coefficients a_i and b_i are defined by

$$a_i = \frac{2}{T} \cdot \int_0^T f_1(t) \cdot \cos(i\omega t) dt \tag{24}$$

$$b_i = \frac{2}{T} \cdot \int_0^T f_1(t) \cdot \sin(i\omega t) dt \tag{25}$$

Bearing this in mind, it is easy to conclude that the modified two-channel SDMM can be used for measurement of the coefficients a_i and b_i [8]. For that purpose it is necessary to replace the analog sum of the signals $f_2(t)$ and h_2 by memorized two-bit samples of a dithered (co)sine wave (Fig. 6). For instance, if $f_2(t) = R_2 \cdot \cos(j\omega t) = R \cdot \cos(j\omega t)$, the output value $\bar{\Psi}$ will be equal to

$$\bar{\Psi} = \frac{1}{N} \cdot \sum_{i=1}^{N} \Psi_1(i) \cdot \Psi_2(i) \approx \frac{1}{t_2 - t_1} \cdot \int_{t_1}^{t_2} f_1(t) \cdot R_2 \cdot cos(j\omega t)\, dt = \frac{R}{2} \cdot a_i \tag{26}$$

Analogously, if $f_2(t) = R_2 \cdot \sin(j\omega t) = R \cdot \sin(j\omega t)$, the instrument's output value will be equal to [8]

$$\bar{\Psi} = \frac{1}{N} \cdot \sum_{i=1}^{N} \Psi_1(i) \cdot \Psi_2(i) \approx \frac{1}{t_2 - t_1} \cdot \int_{t_1}^{t_2} f_1(t) \cdot R_2 \cdot sin(j\omega t)\, dt = \frac{R}{2} \cdot b_i \tag{27}$$

From (16) it is easy to show that the variance of the average error *e* will not be greater than [16]

$$\sigma_{\bar{e}}^2 \le \frac{1.87^2}{8} \cdot \frac{R^2}{N} \tag{28}$$

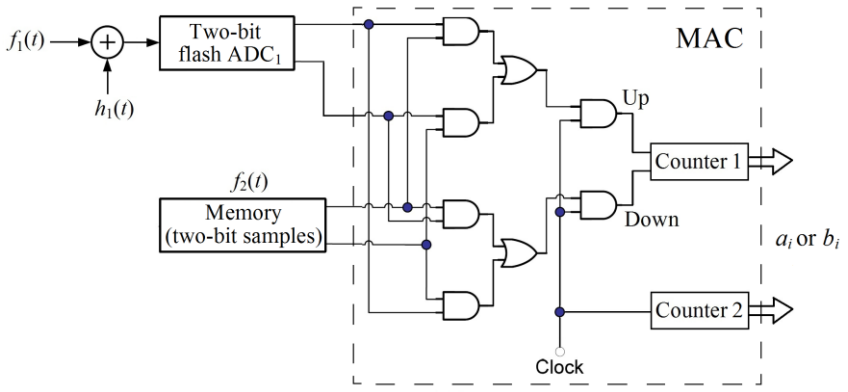

Fig. 6. A two-bit scheme for measurement one Fourier coefficient.

Since in this case a MAC (multiply and accumulate) block also processes two-bit samples, its structure is extremely simple [16]. More precisely, it consists only of two counters and few logic gates (Fig. 6). The content of Counter 1 represents the sum of the product of two-bit samples, while the content of Counter 2 shows the number of measurement cycles in the interval $t_2 - t_1$. Obviously, if we want to measure M Fourier coefficients, we need to use $2M$ memory blocks, $2M$ MAC blocks, $2M$ Counters 1 and (usually) one Counter 2 (Fig. 7). The microprocessor is in charge of dividing the content of Counter 1 with the content of Counter 2. In this way one obtains Fourier coefficients, i.e.

$$a_i = \frac{2 \cdot <\text{Counter}\,1_{2i-1}>}{<\text{Counter}\,2_{2i-1}>} \tag{29}$$

$$b_i = \frac{2 \cdot <\text{Counter}\,1_{2i}>}{<\text{Counter}\,2_{2i}>} \tag{30}$$

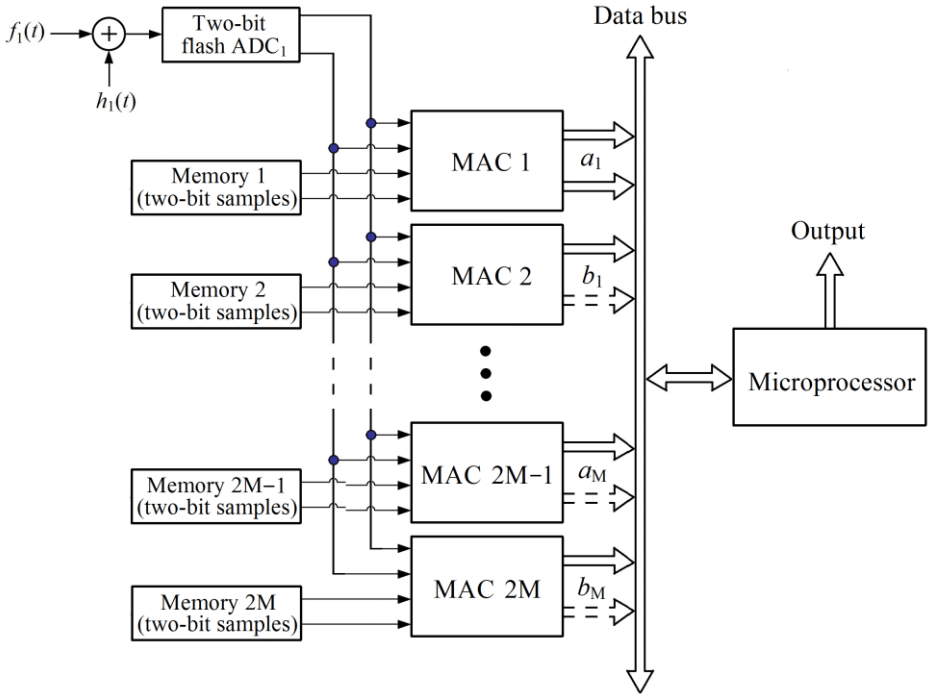

Fig. 7. A two-bit stochastic DFT processor for measurement $2M$ Fourier coefficients.

3.2. Electrical Quantities and Fourier Coefficients

The above described processor can be used for various kinds of measurements. One of the most challenging applications is the measurement of electrical quantities in a power grid network. By knowing them, the utility companies can take the proper steps to reduce revenue losses and increase the power generation capacity. Given this, suppose that the voltage and current signals, $u(t)$ and $i(t)$, are accurately approximated with M-order trigonometric polynomials

$$u(t) \approx \frac{a_0}{2} + \sum_{i=1}^{M} [a_i \cdot \cos(i\omega t) + b_i \cdot \sin(i\omega t)] \tag{31}$$

$$i(t) \approx \frac{c_0}{2} + \sum_{i=1}^{M} [c_i \cdot \cos(i\omega t) + d_i \cdot \sin(i\omega t)] \tag{32}$$

The main parameter that is measured in both cases is the effective value of the signal. Its definition in continuous case is:

$$U_{eff.} = \sqrt{\frac{1}{T} \cdot \int_0^T u^2(t)\, dt} \tag{33}$$

$$I_{eff.} = \sqrt{\frac{1}{T} \cdot \int_0^T i^2(t)\, dt} \tag{34}$$

or, using Fourier coefficients [12]

$$U_{eff.} = \sqrt{\frac{a_0^2}{4} + \sum_{i=1}^{M} \left(\frac{a_i^2 + b_i^2}{2} \right)} \tag{35}$$

$$I_{eff.} = \sqrt{\frac{c_0^2}{4} + \sum_{i=1}^{M} \left(\frac{c_i^2 + d_i^2}{2} \right)} \tag{36}$$

The ideal situation in the power grid is when both current and voltage are sinusoidal. The real situation is different, and the parameter that defines the difference between the real and ideal situation is THD factor (THD - Total Harmonic Distortion). It is indicated often with THD and is defined by the following equation [12]:

$$\mathrm{THD}_u = \sqrt{\frac{\sum_{i=2}^{M} \left(a_i^2 + b_i^2 \right)}{a_1^2 + b_1^2}} \tag{37}$$

$$\mathrm{THD}_i = \sqrt{\frac{\sum_{i=2}^{M} \left(c_i^2 + d_i^2 \right)}{c_1^2 + d_1^2}} \tag{38}$$

The first important combined complex periodic quantity is the active power. In analog domain it is defined by

$$P = \frac{1}{T} \cdot \int_0^T u(t) \cdot i(t)\, dt \tag{39}$$

In accordance with the foregoing, it can be shown that [12]

$$P = \frac{a_0 \cdot c_0}{4} + \frac{1}{2} \cdot \sum_{i=1}^{M} (a_i \cdot c_i + b_i \cdot d_i) \tag{40}$$

is active power expressed using Fourier coefficients of voltage and current.

The second important combined complex periodic quantity is the reactive power. In analog domain it is calculated by

$$Q = \frac{1}{T} \cdot \int_0^T u(t - \frac{T}{4}) \cdot i(t)\, dt \tag{41}$$

while using Fourier coefficients it can be computed as follows [12]

$$Q = \frac{1}{2} \cdot \sum_{i=1}^{M} \left[(a_i \cdot c_i + b_i \cdot d_i) \cdot cos(-i \cdot \frac{\pi}{2}) + (b_i \cdot c_i - a_i \cdot d_i) \cdot sin(-i \cdot \frac{\pi}{2}) \right] \tag{42}$$

The third important combined complex periodic quantity is the apparent power which is usually denoted by *S*. Apparent power is defined as the product of the effective values of voltage and current. Definitional relation of reactive power in the analog domain is

$$S = \sqrt{\frac{1}{T} \cdot \int_0^T u^2(t)\, dt} \cdot \sqrt{\frac{1}{T} \cdot \int_0^T i^2(t)\, dt} \tag{43}$$

Using Fourier coefficients of the voltage and current, the apparent power can be presented by [12]

$$S = \sqrt{\frac{a_0^2}{4} + \sum_{i=1}^{M} \left(\frac{a_i^2 + b_i^2}{2} \right)} \cdot \sqrt{\frac{c_0^2}{4} + \sum_{i=1}^{M} \left(\frac{c_i^2 + d_i^2}{2} \right)} \tag{44}$$

The last important combined complex periodic quantity is the power factor. It is defined as the ratio of active and apparent power, i.e.

$$PF = \frac{\frac{a_0 \cdot c_0}{4} + \frac{1}{2} \cdot \sum_{i=1}^{M} (a_i \cdot c_i + b_i \cdot d_i)}{\sqrt{\frac{a_0^2}{4} + \sum_{i=1}^{M} \left(\frac{a_i^2 + b_i^2}{2} \right)} \cdot \sqrt{\frac{c_0^2}{4} + \sum_{i=1}^{M} \left(\frac{c_i^2 + d_i^2}{2} \right)}} \tag{45}$$

3.3. Application in Power Systems

In this section, we illustrate a practical application of a two-bit stochastic DFT processor. It is an integral part of the quadruple three-phase power analyzer called MM4 (Fig. 8). This device is able to measure up to 70 quantities:

1) 3 voltage effective values (with the accuracy of 0.2 % of full scale),
2) 16 current effective values (with the accuracy of 0.2 % of full scale),
3) 12 active powers (with the accuracy of 0.5 % of full scale),
4) 38 fundamental Fourier coefficients (with the accuracy of 0.2 % of full scale),
5) power grid frequency (with the accuracy of 0.02 % of full scale).

Fig. 8. A photo of a two-bit quadruple three-phase power analyzer (MM4).

Recently it was used to verify the performances of the conventional measurement equipment (of the 0.2 accuracy class) installed in a big chemical processing plant. The measurements were performed at two second intervals over a period of 500 minutes. The obtained results are shown in Figs. 9-12 and Table 1.

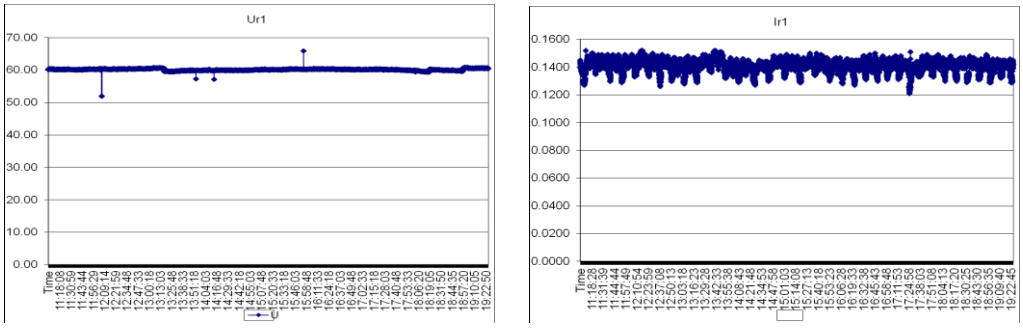

(a) (b)

Fig. 9. The voltage in the R_1-phase (a) and the current in the R_1-phase (b) as functions of time.

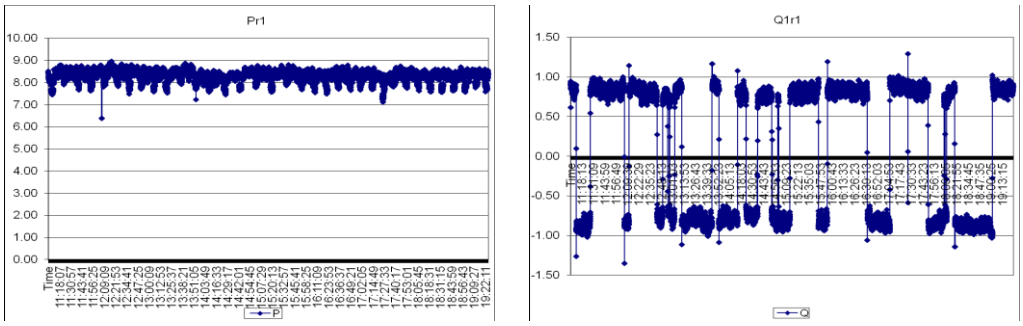

(a) (b)

Fig. 10. The active power in the R_1-phase (a) and the fundamental reactive power in the R_1-phase (b) as functions of time.

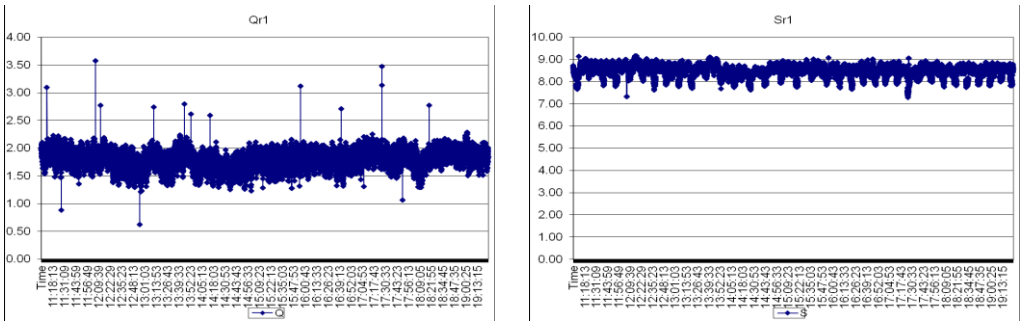

(a) (b)

Fig. 11. Fryze's reactive power in the R_1-phase (a) and the apparent power in the R_1-phase (b) as functions of time.

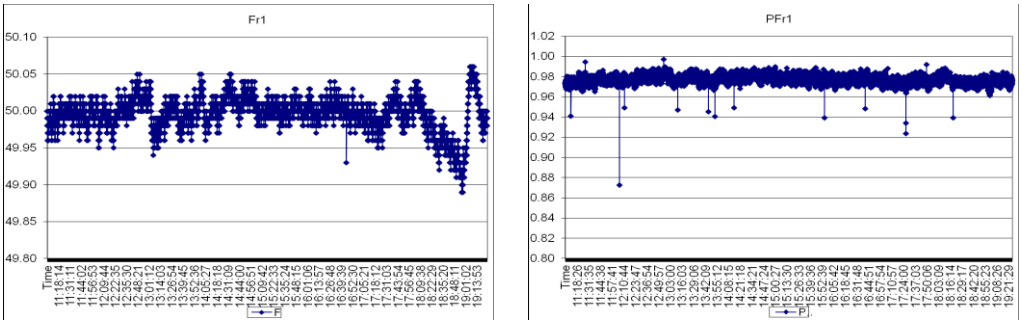

(a) (b)

Fig. 12. The power grid frequency in the R_1-phase (a) and the power factor in the R_1-phase (b) as functions of time.

Table 1. The minimum, average and maximum values of the measured quantities.

	U_{r1} [V]	I_{r1} [A]	P_{r1} [W]	Q_{r1} [var]	Q_{1r1} [var]	S_{r1} [VA]	f_{r1} [Hz]	PF_{r1}
Minimum value	51.93	0.121	6.39	0.62	- 1.35	7.30	49.89	0.873
Average value	60.16	0.141	8.29	1.80	0.10	8.49	50.00	0.977
Maximum value	65.86	0.152	8.96	3.57	1.29	9.16	50.06	0.997
Standard deviation	0.27	0.04	0.25	0.16	0.82	0.25	0.02	0.004

Frize's reactive power (RP) has the highest value of all defined RPs. Today, mainly on Frize's definition, an orthogonal decomposition of apparent power (AP) is performed in several various ways [17-19]. Besides the active power P, in all orthogonal decompositions one of the orthogonal components of AP is Budeanu's RP. In industrial applications the most important component of Budeanu's RP (that at the fundamental frequency) can be easily compensated using parallel capacitive compensators. This is confirmed in this practical case (Fig. 11a and Table 1): the average value of Budeanu's RP at the fundamental frequency is 0.1 var, which is practically negligible.

4. CONCLUSION

In this chapter, we have reviewed the evolution of SDMM with a special emphasis on a two-bit SDMM. It has been shown that SDMM can be used for one-channel, two channel and multi-channel measurements. In the first two scenarios it is possible to measure the average value of the input signal, its absolute mean value, its frequency as well as the mean value of a product of two signals. The third scenario allows us to measure M Fourier coefficients of the input signal. The architecture of the processor that performs this task is extremely simple: it consists of $2M$ memory blocks, $2M$ MAC blocks and $2M + 1$ counters. The mentioned processor is the heart of many prototype instruments, including the quadruple three-phase power analyzer called MM4. In this chapter, it has been shown how this device measures electrical quantities in a grid network by using Fourier coefficients of the voltage and current. In the future, this concept will be extended to the measurement of non-electrical quantities such as wind power and wind energy.

REFERENCES

[1] M. H. Stone, "The Generalized Weierstrass Approximation Theorem," *Math. Mag.*, vol. 21, nos. 4-5, pp. 167–184, pp. 237–254, Mar.–Jun. 1948.

[2] M. F. Wagdy, "Validity of Uniform Error Model for Sinusoidal Signals without and with Dither," *IEEE Trans. Instrum. Meas.*, vol. 38, pp. 718-722, Apr. 1989.

[3] V. Vujicic, S. Milovancev, M. Pesaljevic, D. Pejic and I. Zupunski, "Low Frequency Stochastic True RMS Instrument," *IEEE Trans. Instrum. Meas.*, vol. 48, no. 2, pp. 467-470, Apr. 1999.

[4] D. Pejic and V. Vujicic, "Accuracy Limit of High-Precision Stochastic Watthour Meter," *IEEE Trans. Instrum. Meas.*, vol. 49, no. 3, pp. 617–620, June 2000.

[5] V. Vujicic, "Generalized Low-Frequency Stochastic True RMS Instrument," *IEEE Trans. Instrum. Meas*., vol. 50, pp. 1089–1092, Oct. 2001.

[6] V. Vujicic, I. Zupunski, Z. Mitrovic, M. Sokola, "Measurement in a Point versus Measurement Over an Interval," *Proc. XIX IMEKO World Congress – Fundamental and Applied Metrology*, pp. 1128-1132, Sept. 2009.

[7] B. Santrac, M. Sokola, Z. Mitrovic, I. Zupunski and V. Vujicic, "A Novel Method for Stochastic Measurement of Harmonics at Low Signal-to-Noise Ratio," *IEEE Trans. Instrum. Meas.*, vol. 58, no. 10, pp. 3434–3441, Oct. 2009.

[8] V. Pjevalica and V. Vujicic, "Further Generalization of the Low-Frequency True-RMS instrument," *IEEE Trans. Instrum. Meas.*, vol. 59, no. 3, pp. 736-744, March 2010.

[9] P. Sovilj, S. Milovancev, and V. Vujicic, "Digital Stochastic Measurement of a Nonstationary Signal with an Example of EEG Signal Measurement," *IEEE Trans. Instrum. Meas.*, vol. 60, no. 9, pp. 3230-3232, Sep. 2010.

[10] A. Radonjic, P. Sovilj and V. Vujicic, "Measurement Uncertainty Bounds of DSM Method", *Proc. IEEE Conf. on Precision Electromagnetic Measurements (CPEM) 2012,* pp. 572-573, July 2012.

[11] A. Radonjic, P. Sovilj and V. Vujicic, "Stochastic Measurement of Power Grid Frequency Using a Two-Bit A/D Converter," *IEEE Trans. Instrum. Meas.*, vol. 63, no. 1, pp. 56-62, Jan. 2014.

[12] V. Vujicic, Z. Beljic, P. Sovilj, A. Radonjic and Z. Mitrovic, "Concept of Stochastic Measurements in the Fourier Domain", *Proc. IEEE 16th International Conference on Harmonics and Quality of Power*, pp. 288-292, May 2014.

[13] A. Radonjic, P. Sovilj, V. Vujicic, "Stochastic Measurement in Fourier and Wavelet Domain: a Comparative Study", *Proc. 1st Int. Conf. on Electrical, Electronical and Computing Engineering – IcETRAN 2014*, paper MLI1.3, June 2014.

[14] M. Urekar, A. Radonjic, V. Vujicic, "A Generalized Approach to Stochastic Measurement of Power Grid Frequency", *Proc. 18th Int. Symp. on Power Electronics*, paper T4.1-6, Oct. 2015.

[15] P. Sovilj, B. Vujicic, A. Radonjic, D. Pejic, V. Vujicic, "Stochastic Measurement of Reactive Power Using a Two-bit A/D Converter", *Proc. IMEKO TC-4 Int. Symp. on Understanding the World through Electrical and Electronic Measurement*, pp. 176-179, Sept. 2016.

[16] D. Pejic, D. Naumovic-Vukovic, B. Vujicic, A. Radonjic, P. Sovilj, V. Vujicic, "Stochastic Digital DFT Processor and Its Application to Measurement of Reactive Power and Energy", *Measurement*, vol. 124, pp. 494-504, Aug. 2018.

[17] H. Lev-Ari and A. Stankovic, "A Decomposition of Apparent Power in Polyphase Unbalanced Networks in Nonsinusoidal Operation," *IEEE Trans. Power Systems*, vol. 21, no. 1, pp. 438-440, Feb. 2006.

[18] S. Pajic and A. Emanuel, "Modern Apparent Power Definitions: Theoretical Versus Practical Approach - The General Case," *IEEE Trans. Power Delivery*, vol. 21, no. 4, pp. 1787-1792, Oct. 2006.
[19] L. Czarnecki and P. Haley, "Power Properties of Four-Wire Systems at Nonsinusoidal Supply Voltage," IEEE Trans. Power Delivery, vol. 31, no. 2, pp. 513-521, Apr. 2016.